Cross-linked protein crystals for vaccine delivery

Nancy St. Clair*, Bhami Shenoy*, Lawrence D. Jacob†, and Alexey L. Margolin*‡

*Altus Biologics Inc., 625 Putnam Avenue, Cambridge, MA 02139; and †Inveresk Research, Tranent EH33 2NE, Scotland

ABSTRACT   The progress toward subunit vaccines has been limited by their poor immunogenicity and limited stability. To enhance the immune response, subunit vaccines universally require improved adjuvants and delivery vehicles. In the present paper, we propose the use of cross-linked protein crystals (CLPCs) as antigens. We compare the immunogenicity of CLPCs of human serum albumin with that of soluble protein and conclude that there are marked differences in the immune response to the different forms of human serum albumin. Relative to the soluble protein, crystalline forms induce and sustain over almost a 6-month study a 6- to 10-fold increase in antibody titer for highly cross-linked crystals and an approximately 30-fold increase for lightly cross-linked crystals. We hypothesize that the depot effect, the particulate structure of CLPCs, and highly repetitive nature of protein crystals may play roles in the enhanced production of circulating antibodies. Several features of CLPCs, such as their remarkable stability, purity, biodegradability, and ease of manufacturing, make them highly attractive for vaccine formulations. This work paves the way for a systematic study of protein crystallinity and cross-linking on enhancement of humoral and T cell responses.

Subunit vaccines that consist of well characterized molecules are extremely attractive due to their superior safety profile and ease of manufacturing via chemical synthesis or recombinant DNA technology. However, the price one has to pay for these advantages is significant: subunit vaccines are generally poorly immunogenic and in many cases cannot compete with attenuated and inactivated counterparts (1). Thus, the formulation of antigens with adjuvants, compounds that augment the immune response, is necessary. Unfortunately, alum (mixture of aluminum salts and aluminum hydroxide), the only adjuvant currently approved for human use, is a weak potentiator of the immune response. Other adjuvants, such as Freund's adjuvants, are much stronger but are often toxic. In addition, most conventional adjuvants, although providing enhanced neutralizing antibody titer, fail to elicit an antigen-specific cytotoxic T lymphocyte (CTL) response (2). Not surprisingly, in recent years significant effort has been focused on development of safe and efficacious adjuvants (3) that enhance the immune response by stimulating the immune system directly and/or by affecting the presentation of antigen to the immune system (4). Significant enhancement of the immune response can be achieved by using liposomes (5); oil-in-water emulsions composed of Pluronic, squalane, and Tween (6); immunostimulating complexes (7); QS-21 (8); and polymeric microspheres (9).

Another challenge to successful subunit vaccine design and development comes from the poor stability of antigens and adjuvants. Aqueous single-vial vaccines, which are ready to use and can be stable under storage without refrigeration, are highly desirable but are difficult to formulate due to the physical and chemical instability of the proteins. In fact, antigen stability during manufacturing, storage, and release is one of the most serious obstacles for successful immunization using polymeric microspheres (10). The development of lyophilized vaccines, on the other hand, requires significant efforts and may not always be possible because the process requirements for freezing and drying of antigens and adjuvants may be radically different. Alum, for example, cannot be lyophilized due to the instability of its particles during freezing (11).

To alleviate the acute need for stable and efficacious subunit vaccines novel ideas and different approaches may be necessary. We hypothesized that many problems related to the immunogenicity and stability of subunit vaccines may be solved by using cross-linked protein crystals (CLPCs) as antigens. Indeed, several major features of protein crystals make them highly attractive for vaccine formulations. (*i*) Protein crystals are ultimately biodegradable; can be produced in a variety of sizes, shapes, and forms (12); and are well suited to investigate the effect of the physical nature of the immunogen on the immune response. (*ii*) Protein crystals by definition are very pure, can currently be produced on large scale (13), and do not require cumbersome manufacturing processes used for the preparation of synthetic microspheres. (*iii*) CLPCs are remarkably stable (13) at elevated temperature, in organic and mixed solvents, and against mechanical disruption and shear (14–17). (*iv*) Because the degree of cross-linking can be manipulated by the concentration of the cross-linking agent, time of reaction, and the reaction conditions, one can produce a variety of CLPCs with different dissolution profiles. In short, CLPCs constitute a type of biodegradable microparticulates with high-porosity, pore surface area, and a wide range of pore size (17).

Despite the obvious advantages of CLPCs, there have been only a few reports to date on immunogenicity of crystals in general (18, 19) and protein crystals in particular (20). The perceived difficulties of protein crystal preparation have been a major stumbling block in exploring the field. To be useful as subunit vaccines, not only do protein crystals have to be available in quantity, they have to exhibit relatively low solubility at the injection site. Both these conditions are hard to achieve with un-cross-linked protein crystals. When these conditions are met, however, the results can be very encouraging. For example, Wade-Evans *et al.* (21) have found that crystals of the major outer core protein of African horsesickness virus (AHSV), VP7, that spontaneously crystallized in the course of virus purification were effective as a vaccine against lethal doses of AHSV in mice.

To the best of our knowledge, the immunogenicity of CLPCs has never been studied. Herein we compare the immunoge-

Abbreviations: CLPC, cross-linked protein crystal; lCLPC, lightly cross-linked protein crystals; hCLPC, heavily cross-linked protein crystals; HSA, human serum albumin; CTL, cytotoxic T lymphocyte; FIA, Freund's incomplete adjuvant; VLP, virus-like particle.
‡To whom reprint requests should be addressed. E-mail: margolin@altus.com.

nicity of CLPCs of human serum albumin (HSA) with that of soluble protein. We conclude that cross-linked protein crystals have a profound self-adjuvanting effect, comparable with that of Freund's incomplete adjuvant (FIA).

MATERIALS AND METHODS

Materials. HSA, rabbit anti-human IgG, horseradish peroxidase-conjugated goat anti-rabbit IgG, PBS with Tween 20, phosphate-citrate buffer with sodium perborate, bovine nonfat dried milk, tetramethylbenzidine dihydrochloride tablets, anti-rat IgG peroxidase conjugate, carbonate–bicarbonate buffer capsule, PBS tablet, and monoclonal anti-HSA clone were products of Sigma.

CNBr-activated Sepharose 4B was from Pharmacia, A/G Plus-Agarose Affinity System was from Calbiochem, and glutaraldehyde was from Aldrich. All other reagents were of analytical grade or purer and obtained from commercial suppliers.

HSA Crystallization. Five grams of lyophilized HSA was added gradually to a 30-ml stirred solution of 50 mM K/Na phosphate buffer (pH 6.3). After the protein was solubilized, the solution was brought to a final volume of 50 ml with phosphate buffer. Final HSA concentration was 100 mg/ml. All subsequent manipulations were performed at 4°C. After cooling to 4°C the protein solution was brought to 2.5 M saturated ammonium sulfate by the addition of 50 ml of 4 M ammonium sulfate with stirring. The solution became hazy upon addition of ammonium sulfate. Small needle/rod-shaped crystals began to appear within 2 h. The solution was allowed to stir at 4°C for 24 h. Crystals (1–5 μm) were recovered by centrifugation. The crystals were washed twice with 50 ml of ice-cold 2.5 M ammonium sulfate containing 50 mM K/Na phosphate (pH 6.3). To determine the yield of crystallization, the recovered crystals were solubilized in water and protein concentration was determined with the Pierce BCA protein assay according to the manufacturers instructions. Approximately 80% of the protein was in crystal form.

Cross-Linking. *Preparation of lightly cross-linked CLPCs (lCLPCs).* A 10-ml slurry of HSA crystal (100 mg/ml) containing 50 mM K/Na phosphate (pH 6.3) and 2.5 M ammonium sulfate was cross-linked for 1 h at 4°C with 1% (final concentration) glutaraldehyde as supplied by the manufacturer. The pH of the cross-linking reaction was maintained between pH 6.0 and 6.3 by addition of 250 mM NaOH. The 25% glutaraldehyde stock was stored at −20°C before use. The 25% glutaraldehyde stock was diluted to 12.5% with water immediately before addition to the protein. After cross-linking, the HSA lCLPCs were diluted with 90 ml of phosphate-buffered 2.5 M ammonium sulfate and recovered by vacuum filtration. The lCLPCs were then resuspended twice in 50 ml of phosphate-buffered ammonium sulfate and recovered by filtration. Between recoveries, each wash was allowed to incubate for >1 h with rocking. Absorbance at 280 nm in the supernatant after the second wash was 0. After washing in buffered ammonium sulfate, the crystals were transferred to 2.5 M sodium/potassium phosphate (K/Na phosphate) buffer (pH 6.3). A K/Na phosphate buffer was prepared by adding 2.5 M K$_2$HPO$_4$ to 2.5 M NaH$_2$PO$_4$·H$_2$O to pH 6.3 at 4°C.

Preparation of heavily cross-linked CLPCs (hCLPCs). The cross-linking method described for the preparation of lCLPCs was followed with the following modifications. The final concentration of glutaraldehyde was 5%. The cross-linking was allowed to proceed for 3 h. The glutaraldehyde was pretreated with sodium borate and heat before addition to protein. Both hCLPC and lCLPC were stored at 4°C.

Crystal Morphology. The crystal integrity of the formulations was measured by quantitative microscopic observations and by particle size distribution with a Coulter particle size analyzer. Similar size was obtained by microscopic examina-

tion using IMAGEPRO software. An Olympus BX60 microscope equipped with DXC-970MD 3CCD color video camera with camera adapter with IMAGE PROPLUS software (Media Cybernetics, Silver Spring, MD) was used for microscopic observations.

Secondary Structure Characterization by Fourier Transform–IR Spectroscopy (FTIR). The FTIR spectra were collected on a Nicolet model 560 Magna series spectrometer as described by Dong *et al* (22). The HSA slurry sample of about 1 ml was placed on a Zinc selenide crystal of Attenuated Total Reflectance kit Enhanced Synchronization Protocol (ARK ESP). The spectra were collected and then processed with GRAMS 32 from Galactic software for the determination of relative areas of the individual components of secondary structure by using the second derivative and curve-fitting program under the amide I region (1,600–1,700 cm^{-1}).

Amino Acid Analysis. The number of lysine residues in CLPCs was determined by amino acid analysis. Amino acid analysis was done by reverse-phase HPLC with precolumn derivatization with phenyl isothiocyanate as described by Heinrikson and Meredith (23).

Immunogenicity Studies in Rats. *Dose groups and sample collection.* Female Sprague–Dawley rats (180–200 g) were obtained from Charles River and housed five rats to a cage. The room environment was maintained at 20 ± 2°C and 50 ± 15% humidity with 15–20 air changes per hour. Animals were fed with rat and mouse no. 1 Expanded diet (special diet services) provided ad libitum. One control group (group 1) and six dose groups (five rats per group) were used in the study. Each dose group was subcutaneously immunized with 50 μg (not more than 0.2 ml) of soluble HSA (group 2), soluble HSA + FIA (group 3), lCLPC (group 4), lCLPC + FIA (group 5), hCLPC (group 6), and hCLPC + FIA (group 7) at days 1 and 29 of the study. The samples in PBS were emulsified with FIA by mixing until a stable continuous white emulsion was formed. This was further mixed by using a magnetic flea immediately before subcutaneous injection under the dorsal skin. Blood samples of approximately 1 ml were collected at days 1, 11, 33, 40, 54, 68, 82, 119, and 167 into glass tubes and allowed to coagulate. The clot was allowed to contract overnight at 4°C before centrifugation and placing the serum into 1.7-ml labeled Eppendorf tubes. The serum was stored at −70°C to −20°C before analysis. Five animals from groups 2 and 4 were bled under terminal anesthesia at day 40 and serum was used in the immunoabsorption experiments.

Preparation of HSA immobilized on Sepharose 4B (HSA-Sepharose). HSA was attached to CNBr-activated Sepharose 4B according to the manufacturers instruction. A total of 68 mg of HSA was attached per 2 g of resin. The resin was stored at 4°C in PBS until use.

Absorption of serum using HSA-Sepharose. Pooled serum obtained from animals of dose groups 2 and 4 was diluted 1:10 with PBS and absorbed against HSA-Sepharose, a total of 0.9 ml of diluted serum was mixed with 0.6 ml of resin. The serum and resin were mixed by end-over-end inversion. Aliquots of 0.75 ml of mixture were removed immediately and after 60 min. The resin was separated from the serum immediately after removal and before analysis. A control of diluted rabbit anti-HSA was also included to check the effectiveness of the absorption. After absorption, the titer of antibody remaining was assayed in a plate bound soluble HSA assay and a plate bound hCLPC HSA assay.

Determination of the titer of circulating antibodies. The titer of circulating antibodies was determined as follows. The wells of a 96-well ELISA plate were filled with 100 μl of HSA (10 μg/ml) in PBS and incubated overnight at about 4°C. After incubation, the plate was washed three times with PBS/Tween 20, 0.05% (vol/vol), and then blocked by incubating at room temperature for 1–2 h after the addition of 200 μl of 3% (wt/vol) nonfat dried milk in PBS/Tween 20 to each well. The
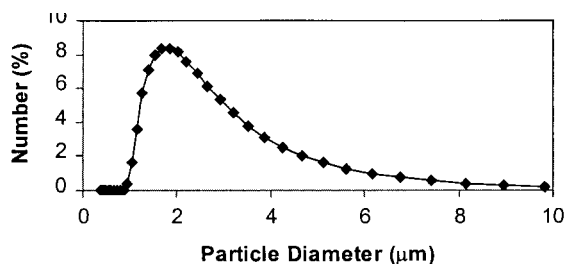
FIG. 1. lCLPC–HSA size distribution determined with a Coulter counter. The size distribution of hCLPC and uncross-linked HSA crystals is similar.

plate was washed three times as above. The wells were filled with 50 μl of PBS except for those wells in column 2, which were filled with the test serum prediluted in PBS. Column 1 contained 50 μl of PBS as a blank. The test serum was serially diluted by the transfer of 50 μl of the diluted serum into adjacent columns, discarding the extra 50 μl from the last column. Antibody binding was allowed to proceed by incubation overnight at 4°C. Excess antibody was removed by washing three times as above. The presence of bound antibody was detected by incubation at room temperature for 1 h with 50 μl per well of goat anti-rat IgG peroxidase-conjugate diluted 1:19,000 in PBS. Excess antibody was removed by washing and the conjugate was detected by the addition of tetramethylbenzidine. The reaction was stopped by the addition of 1.0 M sulfuric acid at 50 μl per well, and the absorbance at 450 nm was read. The blank (column 1) absorbance was subtracted, and the antibody titer was determined as the highest dilution of antibody that gave an absorbance greater than 0.1.

This assay was also used for measuring the titer of antibodies remaining after immunoabsorption. The assay performed with plate bound hCLPC–HSA was identical except that at step 1, where hCLPC–HSA (25 μg/ml) in carbonate–bicarbonate buffer (pH 9.0) was used.

RESULTS

Characterization of CLPC–HSA. The number average size of HSA crystals determined with a Coulter counter was around 2.7 μm. The cross-linking of crystals does not change the size and microscopic appearance of crystals (Figs. 1 and 2) despite the fact that, of 59 Lys residues per mol of HSA, 42 and 50 residues were modified in lCLPC–HSA and hCLPC–HSA, respectively.

The effect of cross-linking on the secondary structure of crystalline HSA has been studied by FTIR spectroscopy. The
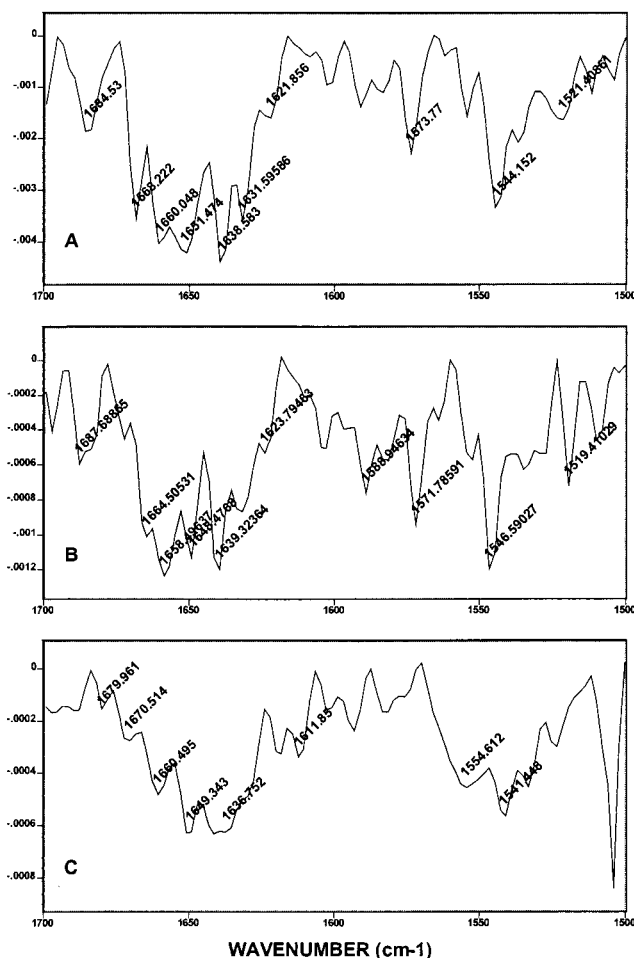

FIG. 2. Microphotograph of lCLPC. (×5,000).

FIG. 3. Second derivatives of FTIR spectra of soluble HSA (*A*), lCLPC (*B*), and hCLPC (*C*) in the amide I region, taken at room temperature. The tentative assignments areas follows: 1,621 (β-structure), 1,631 (β-structure), 1,636–1,638 (β-structure), 1,648–1,649 (random), 1,651–1,659 (α helix), 1,660–1,664 (β-structure), 1,678–1,679 (β-turn), and 1,684–1,687 (β-structure).

second derivative of FTIR spectra of uncross-linked crystals, lCLPC–HSA and hCLPC–HSA were compared in the amide I region after area normalization and curve fitting (Fig. 3). The band positions and their assignments were made as described by Dong *et al.* (22). The secondary structure calculations showed that modification of the first 42 Lys residues (lCLPC–HSA) does not change α-helix content (23%) but leads to an increase of random coil structure (11%). The further cross-linking, however, (hCLPC–HSA) reduces the α-helix content to 12% and further raises the random structure to 26% (Table 1).

Formation of New Epitopes by Crystallization and Cross-Linking. To determine whether new epitopes were formed as a result of crystallization and cross-linking, hCLPC–HSA and soluble HSA at day 40 were incubated with HSA immobilized on Sepharose beads. The immobilized HSA should remove all antibodies to epitopes found on soluble HSA; therefore, it would be expected that no, or very few, HSA-specific anti-

Table 1. Secondary structure contents for CLPC and soluble HSA

Sample	α-helix, %	β-structure, %	β-turn, %	Random, %
Soluble HSA	25	66	9	—
lCLPC–HSA	23	61	5	11
hCLPC–HSA	12	57	5	26

Table 2.   Immunoabsorption on HSA–Sepharose

Antigen	Plate coating	Antibody titer before immunoabsorption	Antibody titer at 0-min absorption*	Antibody titer at 60-min absorption
Rabbit anti-HSA[†]	HSA	2.56×10^6	1.62×10^5	$<2.0 \times 10^4$
	hCLPC–HSA	1.28×10^6	NA	NA
HSA	HSA	2.5×10^4	3.2×10^2	6.0×10^1
	hCLPC–HSA	3.2×10^3	1.0×10^1	$<1.0 \times 10^1$
hCLPC–HSA	HSA	2.56×10^4	3.2×10^2	2.0×10^1
	hCLPC–HSA	3.2×10^3	1.0×10^1	$<1.0 \times 10^1$

Experiments were performed in duplicate. NA, not applicable.
*Sample was removed immediately after mixing.
[†]Control antiserum.

bodies should remain after such treatment. If the new epitopes were present in the hCLPC–HSA, then antibodies to these new epitopes that failed to be absorbed on the column would be detected in the ELISA with plate bound hCLPC–HSA. The experimental results presented in Table 2 demonstrate that HSA-Sepharose efficiently absorbs the rabbit anti-HSA antibodies, used as control, as well as antibodies formed in responses to immunization by soluble HSA and hCLPC–HSA. No evidence was seen of a significant antibody titer remaining in the hCLPC–HSA-immunized rat sera compared with that seen in the soluble HSA-immunized rat sera. On the basis of this experiment, we conclude that there is no evidence of new epitope formation as a consequence of the crystallization and cross-linking process.

Enhancement of the Antibody Response to HSA. To determine the degree of the immune response to the protein crystals, one control group and six dose groups of rats (five rats per group) were subcutaneously immunized with 50 μg of soluble HSA, soluble HSA + FIA, lCLPC, lCLPC + FIA, hCLPC, and hCLPC + FIA at day 1 and 29 of the study. Plasma samples were collected from the tail vein at certain times, and the titer of circulating antibodies was determined by ELISA.

Plots of the mean titer of anti-HSA antibodies for a soluble HSA and two crystalline forms of HSA without adjuvant are presented in Fig. 4. The results indicate that there are marked differences in the immune response to the different forms of HSA. Relative to the soluble protein, crystalline forms induce a 6- to 10-fold increase in antibody titer for hCLPC and an approximately 30-fold increase for lCLPC sustained over an almost 6-month study. The addition of FIA further stimulates (5- to 7-fold) the immune response of all samples (Fig. 5). Once again lCLPC demonstrates the highest titer; however, in the presence of FIA, the difference between lCLPC and soluble HSA is small (less than 2-fold).

DISCUSSION

In this paper, we have demonstrated that cross-linked crystals of HSA are significantly more immunogenic than soluble protein when injected subcutaneously in rats. The magnitude of the immune response depends on the degree of crystal cross-linking (Figs. 4 and 5). In fact, the immunogenicity of lightly cross-linked HSA crystals, as judged by the circulating antibody titer, comes close to that of the combination of soluble HSA and FIA, one of the strongest adjuvants available. Three major phenomena—a depot effect, the particulate nature of antigens, and the highly repetitive structure of epitopes in protein crystals—may be responsible for enhanced immunogenicity of protein crystals.

It is well accepted that the slow release of antigen from the site of injection prolongs the time for interaction between antigen and antigen presenting cells and lymphocytes. This depot effect can be achieved by adsorbing antigens on aluminum salts or by including them in the water-in-mineral oil emulsions (FIA), liposomes, or polymeric microspheres. The superior adjuvanticity of FIA over alum in many cases was explained in part by more prolonged release of antigen (24). Several polymeric microspheres can deliver antigen in a continuous or even pulsatile fashion, thus mimicking the administration of traditional bolus and booster immunizations (9). However, the depot effect alone cannot explain many effects of adjuvants mode of action (25). It is well established that the heterogeneous or particulate nature of antigens increases the likelihood of phagocytosis. Both aluminum adjuvants (particle size <10 μm) (26) and water-in-oil emulsions cause inflammation at the site of injection, attracting immunocompetent cells and forming a granuloma. The effect of particle size of the biodegradable polylactic coglycolic acid microspheres on the immune response against staphylococcal enterotoxin B toxoid was studied by Eldridge *et al* (27). Small antigen-containing microspheres (1–10 μm) exhibited 10 times stronger adjuvant
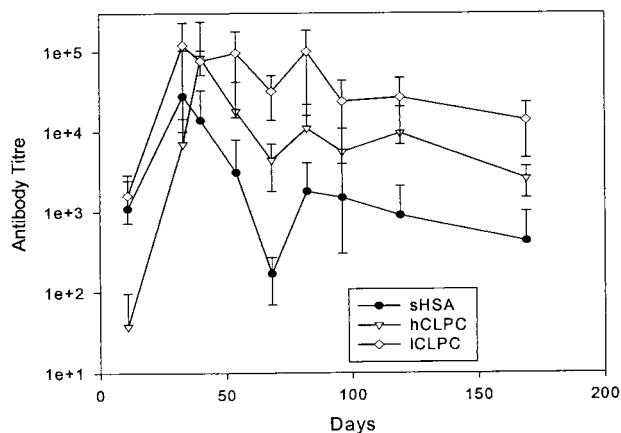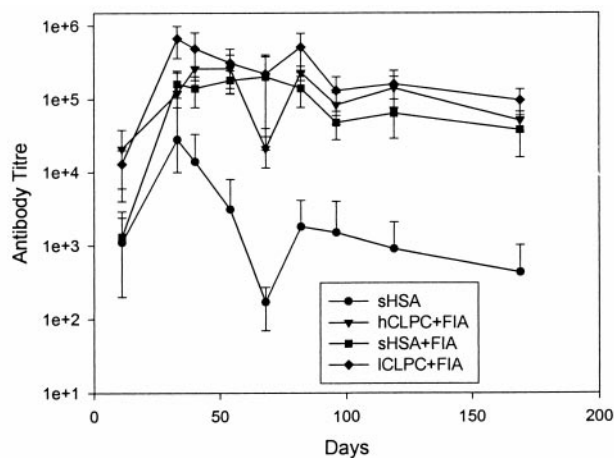

FIG. 4.   Mean antibody titer developed in the absence of FIA. The apparent asymmetry of the position of the arithmetic mean within the error bars is due to the logarithmic scale.

FIG. 5.   Mean antibody titer developed in the presence of FIA.

activity than large particles (>10 μm). This effect correlated with the delivery of smaller microspheres into the draining lymph nodes within macrophages. At the same time, the intraperitoneal injection into mice of the mixture of the 1- to 10-μm and 20- to 50-μm microspheres elicited a much stronger secondary immune response than either size range alone or than with alum (28). These experiments convincingly demonstrate the concerted mechanism of adjuvant action. Small particles are actively taken by macrophages to generate primary antibody response. Larger particles, which cannot be phagocytosized, provide for long-term depot effect and thus stimulate strong secondary antibody response.

It is very likely that both the depot effect and the particulate structure of CLPC play a significant role in the enhancement of the humoral immune response. The small size of CLPC used in this study (mean size 2 μm; Fig. 1) may facilitate their uptake by antigen-presenting cells to promote the primary antibody response over that of soluble HSA. At the same time, the difference between the effect of lCLPC and hCLPC (Fig. 4) may be due to the differences in the protein release profile. The higher concentration of glutaraldehyde and longer cross-linking time result in a higher degree of modification of Lys residues (42 in lCLPC vs. 50 in hCLPC). The longer cross-linking significantly affects the protein release from a crystal. When a suspension of hCLPC at 20 mg/ml was incubated at 37°C in PBS with rapid stirring, the protein leaching was less than 0.2% over a 72-h period. Under the same conditions, protein release from lCLPC reaches 17% in the first 72 h and then levels off. Although the composition of extracellular fluids and cytoplasm is more aggressive than PBS and most certainly leads to degradation of even highly cross-linked crystals, it is possible that a certain "optimal" level of cross-linking results in a better release profile and thus higher immunogenicity. The loss of the HSA secondary structure in hCLPC (reduction of α-helix and increase of random coil; Table 1) can also contribute to the differences between lCLPC- and hCLPC-stimulated immune responses.

One significant difference between CLPC and other forms of antigens used to date is the physical nature of antigens—CLPC are crystalline, whereas all other antigens are amorphous. Protein crystals present highly concentrated and highly ordered structures (29). The solvent content of typical protein crystals is composed of uniform solvent-filled channels that ranges from 30% to 65% of the total crystal volume (30). For example, the porosity of CLPC–HSA was determined to be 65% (17). The appearance of a macroscopic protein crystal containing roughly 10^7–10^{15} molecules begins with formation of small but stable nuclei (30–40 molecules) whose intermolecular contacts are similar to those found in the final crystal. The highly repetitive structure of a protein crystal results in multiple copies of the antigen presented to the immune system as a part of a relatively large particle as seen in Fig. 6. In this figure a molecular model of a segment of the three-dimensional lattice of the HSA crystal, produced by crystallization with PEG (32), is shown. The crystal has seven unit cells long each edge; hence, the dimensions of the crystal are 41.2 × 62.2 × 42.5 nm and it contains a total of 686 HSA molecules. Although the crystalline structure of the HSA crystals used in this study may be different (ammonium sulfate was used as a precipitant instead of PEG), one can clearly appreciate the highly ordered structure of crystalline antigens. In this respect CLPC strikingly resemble polyvalent particulate structures of the hepatitis B surface antigen (33), *Helicobacter pylori* urease (34), and virus-like particles (VLP) (35). In the VLPs, antigens are genetically fused to the *TYA* gene, which encodes a particle-forming protein that can self-assemble. For example, several VLPs carrying a variety of structural and regulatory HIV-1 proteins, influenza virus hemagglutinin, bovine and human papillomavirus proteins, and malaria peptides are known (35, 36). The size of these particulates ranges
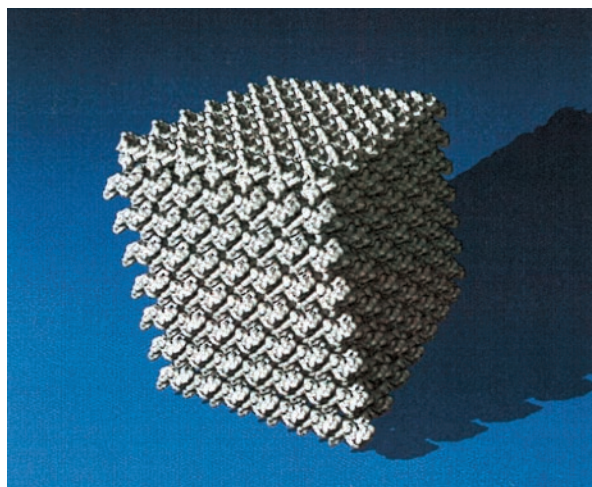

FIG. 6. Computer-generated image of a three-dimensional HSA crystal. The individual enzyme molecules (M_r = 66,000) are shown in silver. The crystal space group is $P2_1$ and the unit cell dimensions are a = 58.86, b = 88.28, and c = 60.68. There are two molecules in the unit cell. Axis a runs across the page, axis b is vertical, and axis c is roughly perpendicular to the page. The surface representation was computed from electron density that was calculated by using atomic coordinates of the reported structure (31) obtained from the Brookhaven Protein Data Bank. A contouring isovalue was chosen to yield a surface whose enclosed volume approximates that of the molecule.

from 10 to 100 nm, with each VLP containing multiple copies of the added immunogen. One of the great advantages of VLPs and other particulates over other forms of antigens is their ability to elicit CTL responses (37). Most conventional vaccines fail to activate a CTL response and thus are ineffective against cancer or virally infected cells (38). It is assumed that effective vaccine delivery requires better targeting of antigen-presenting cells, such as macrophages and dendritic cells. The antigen-presenting cells have the ability to internalize particles into large vacuoles where exogenous antigens are transferred into the class I or II pathways (38, 39). Whereas injection of soluble antigens generally fail to elicit a CTL response, particulates can do it quite efficiently (39, 40). Moreover, it seems that particles larger than viruses can be better presented to macrophages and dendritic cells (39). Given the highly regular structure of protein crystals and the fact that these particles can be produced in different sizes (0.1–100 μm), we believe that CLPCs will be efficient in eliciting CTL immunity.

In conclusion, by using a model protein, we have demonstrated that cross-linked protein crystals have a significant self-adjuvanticity effect in enhancing the humoral immune response. The enhanced immunogenicity of CLPC, combined with their well-established stability, purity, and ease of handling, may open significant opportunities in developing subunit vaccines. This work also poses the following important questions: (*i*) Is self-adjuvanticity of CLPCs a general effect? What is its exact mechanism? In particular, what is the contribution of crystallinity in this effect? (*ii*) Can protein crystals stimulate a CTL response? (*iii*) What is the optimal crystal size and degree of cross-linking?

1. Newman, M. J. & Powell, M. F. (1995) in *Vaccine Design*: *The Subunit and Adjuvant Approach*, eds. Powell, M. F. & Newman, M. J. (Plenum, New York), pp. 1–42.
2. Allsopp, C. E., Plebansky, M., Gilbert, S., Sinden, R. E., Harris, S., Frankel, G., Dougan, G., Hioe, C., Nixon, D., Paoletti, E., *et al.* (1996) *Eur. J. Immunol.* **8,** 1951–1959.

3. Vogel, F. R. & Powell, M. F. (1995) in *Vaccine Design*: *The Subunit and Adjuvant Approach.*, eds. Powell, M. F. & Newman, M. J. (Plenum, New York), pp. 141–228.
4. Kline, D., Hanes, J. & Langer, R. (1996) in *Microparticulate Systems for the Delivery of Proteins and Vaccines*, eds. Cohen, S. & Bernstein, H. (Dekker, New York), pp. 349–379.
5. Gregoriadis, G. (1990) *Immunol. Today* **11**, 89–97.
6. Raychaudhuri, S., Tonks, M., Carbone, F., Ryskamp, T., Mrrow, W. J. & Hanna, N. (1992) *Proc. Natl. Acad. Sci. USA* **89**, 8308–8312.
7. Morein, B., Sundquist, B., Hoglund, S., Dalsgaard, K. & Osterhaus, A. D. M. E. (1984) *Nature (London)* **308**, 457–459.
8. Newman, M. J., Wu, J. Y., Gardner, B. H., Munroe, K. J., Leombruno, D., Recchia, J., Kensil, C. R. & Coughlin, R. T. (1992) *J. Immunol.* **148**, 2357–62.
9. Hanes, J., Cleland, J. L. & Langer, R. (1997) *Adv. Drug Delivery Rev.* **28**, 97–119.
10. Schwendeman, S. P., Cardamone, M., Klibanov, A. M., Langer, R. & Brandon, M. R. (1996) in *Microparticulate Systems for the Delivery of Proteins and Vaccines*, eds. Cohen, S. & Bernstein, H. (Dekker, New York), pp. 1–49.
11. Shirodkar, S., Hutchinson, R. L., Perry, D. L., White, J. L. & Hem, S. L. (1990) *Pharm. Res.* **7**, 1282–1288.
12. McPherson, A. (1989) *Preparation and Analysis of Protein Crystals* (Krieger, Malabar, FL).
13. Margolin, A. L. (1996) *Trends Biotechnol.* **14**, 223–230.
14. Lalonde, J. J., Govardhan, C. P., Khalaf, N. K., Martinez, O. G., Visuri, K. J. & Margolin, A. M. (1995) *J. Am. Chem. Soc.* **117**, 6845–6852.
15. Govardhan, C. & Margolin, A. L. (1995) *Chem. Ind.* 689–693.
16. Persichetti, R. A., St. Clair, N. L., Griffith, J. P., Navia, M. A. & Margolin, A. L. (1995) *J. Am. Chem. Soc.* **117**, 2732–2737.
17. Vilenchik, L. Z., Griffith, J. P., St. Clair, N., Navia, M. A. & Margolin, A. L. (1998) *J. Am. Chem. Soc.* **18**, 4290–4294.
18. Verdier, J.-M., Ewart, K. V., Griffith, M. & Hew, C. L. (1996) *Eur. J. Biochem.,* **241**, 740–743.
19. Perl-Treves, D., Kessler, N., Izhaky, D. & Addadi, L. (1996) *Chem. Biol.* **3**, 567–577.
20. Burroughs, J. N., O'Hara, R. S., Smale, C. J., Hamblin, C., Walton, A., Armstrong, R. & Mertens, P. P. C. (1994) *J. Gen. Virol.* **75**, 1849–1857.
21. Wade-Evans, A. M., Pullen, L., Hamblin, C., O'Hara, R., Burroughs, J. N. & Mertens, P. P. C. (1997) *J. Gen. Virol.* **78**, 1611–1616.
22. Dong, A., Prestrelski, S. J., Allison, S. D. & Carpenter, J. F. (1995) *J. Pharmacol. Sci.* **84**, 415–424.
23. Heinrikson, R. L. & Meredith, S. C. (1984) *Anal. Biochem.* **136**, 65–74.
24. Herbert, W. J. (1976) *Immunology* **14**, 301–318.
25. White, R. G. (1976) *Annu. Rev. Microbiol.* **30**, 579–600.
26. Gupta, R. K., Rost, B. E., Relyveld, E & Siber, G. R. (1995) in *Vaccine Design*: *The Subunit and Adjuvant Approach.*, eds. Powell, M. F. & Newman, M. J. (Plenum, New York), pp. 1–42.
27. Eldridge, J. H., Staas, J. K., Meulbroek, J. A., Tice, T. R. & Gilley, R. M. (1991) *Infect. Immun.* **59**, 2978–2986.
28. Eldridge, J. H., Staas, J. K., Meulbroek, J. A., McGhee, J. R., Tice, T. R. & Gilley, R. M. (1991) *Mol. Immunol.* **28**, 287–294.
29. Weber, P. (1997) *Methods Enzymol.* **276**, 13–22.
30. Matthews, B. W. (1968) *J. Mol. Biol.* **33**, 491–497.
31. He, X. M. & Carter, D. C. (1992) *Nature (London)* **16**, 209–215.
32. Carter, D. C., Chang, B., Ho, J. X., Keeling, K.; Krishnasami, Z. (1994) *Eur. J. Biochem.* **226**, 1049–1052.
33. McAleer, W. J., Buynak, E. B., Maigetter, R. Z. Wampler, D. E., Miller, W. J. & Hilleman, M. R. (1984) *Nature (London)* **307**, 178–80.
34. Austin, J. W., Doig, P., Stewart, M. & Trust, T. J. (1992) *J. Bacteriol.* **174**, 7470–7473.
35. Adams, S. E. & Kingsman, A. S. (1995) in *Vaccine Design*: *The Subunit and Adjuvant Approach.*, eds. Powell, M. F. & Newman, M. J. (Plenum, New York), pp. 769–786.
36. Gilbert, S. C., Plebansky, M., Harris, S. J., Allsopp, C. E., Thomas, R., Layton, G. T. & Hill, A. V. (1997) *Nat. Biotechnol.* **14**, 1280–1284.
37. Sedic, C., Saron, M., Sarraseca, J., Casal, I. & Leclerc, C. (1997) *Proc. Natl. Acad. Sci. USA* **94**, 7503–7508.
38. Tabata, Y. & Ikada, Y. (1988) *J. Biomed. Mater. Res.* **22**, 837–858.
39. Raychaudhuri, S. & Rock, K. L. (1998) *Nat. Biotechnol.* **16**, 1025–1031.
40. Speidel, K., Osen, W., Faath, S., Hilgert, I., Obst, R., Braspenning, J., Momburg, F, Hammerling, G. J. & Rammensee, H. G. (1997) *Eur. J. Immunol.* **27**, 2391–2399.